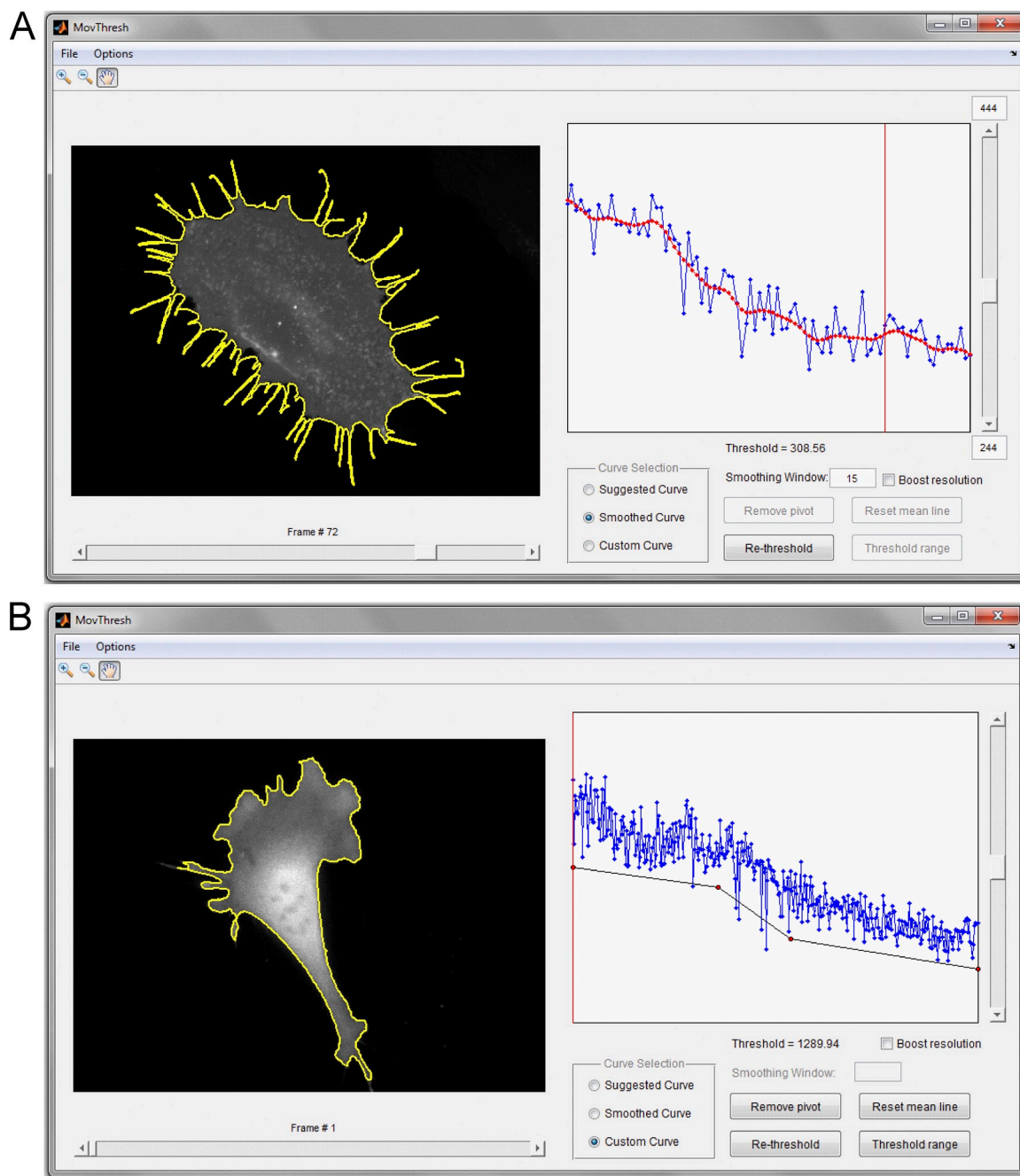Figure S1. **MovThresh module for detecting cell boundary.** (A and B) Two screenshot examples of the GUI. (A) A video of a cell with many filopodia. The blue curve indicates suggested (automatically found) threshold values at each frame. The smoothed curve through the suggested values is shown in red. (B) A long video of 360 frames of a cell with many lamellipodia-like protrusions. The blue curve indicates suggested (automatically found) threshold values at each frame. The black custom curve is produced by manual adjustments in selected time frames (red pivot dots) using two slides: at the bottom (for time) and on the right (for threshold).
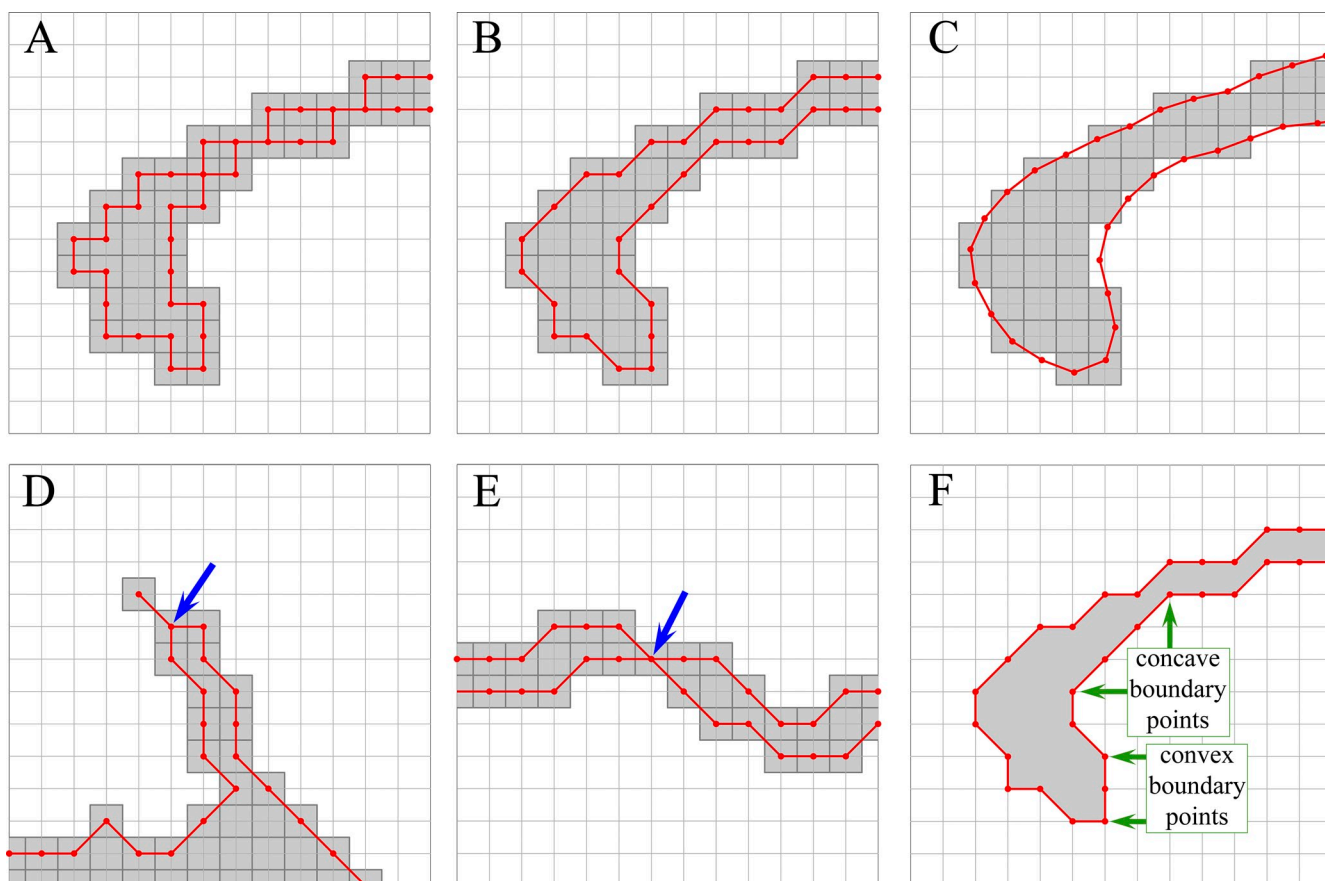
Figure S2. **Examples of boundary representations and self-crossing events.** (A–C) Even the seemingly straightforward task of defining the cell boundary can create ambiguity because of the pixelated nature of digital images. Here, we illustrate examples of different boundary representations (red) of the same object (gray) using four-neighbor tracing (A), eight-neighbor tracing (our default choice; B), and half-maximum level contour of the pixel intensity values smoothed by a Gaussian filter (C). This illustrates why we chose eight-neighbor tracing. (D and E) Examples of self-crossing at 0-width areas of the object (blue arrows). (F) Illustration of the boundary nomenclature.
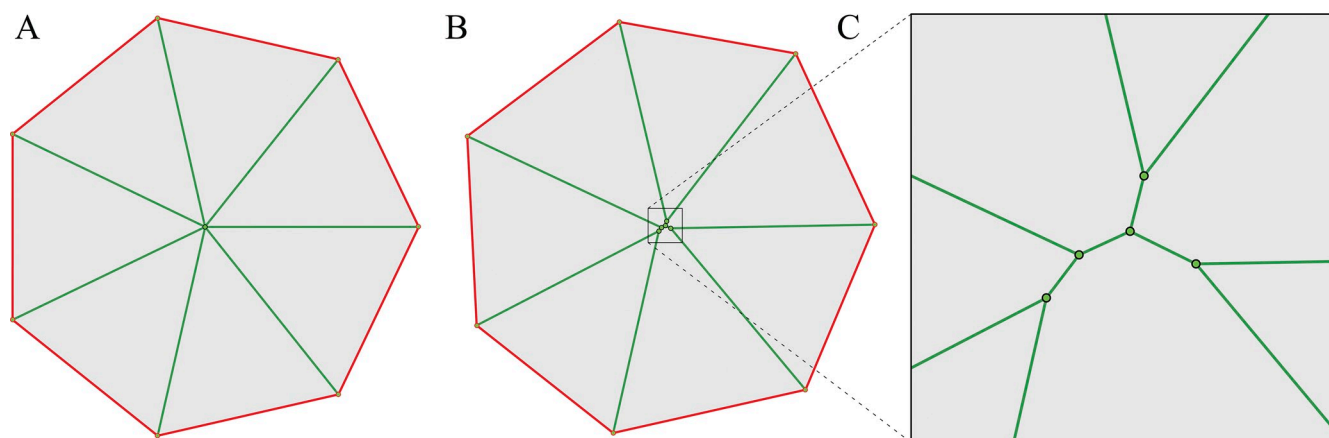

Figure S3. **Examples of degenerate and nondegenerate MATs.** (A) An example of a degenerate MAT (more than three edges at a vertex) of a regular seven-sided polygon. (B) A nondegenerate MAT of a seven-sided polygon after a small random perturbation of the regular one in A. (C) Expanded view of the central region in B, illustrating that each vertex of a nondegenerate MAT is a point where exactly three graph edges meet.
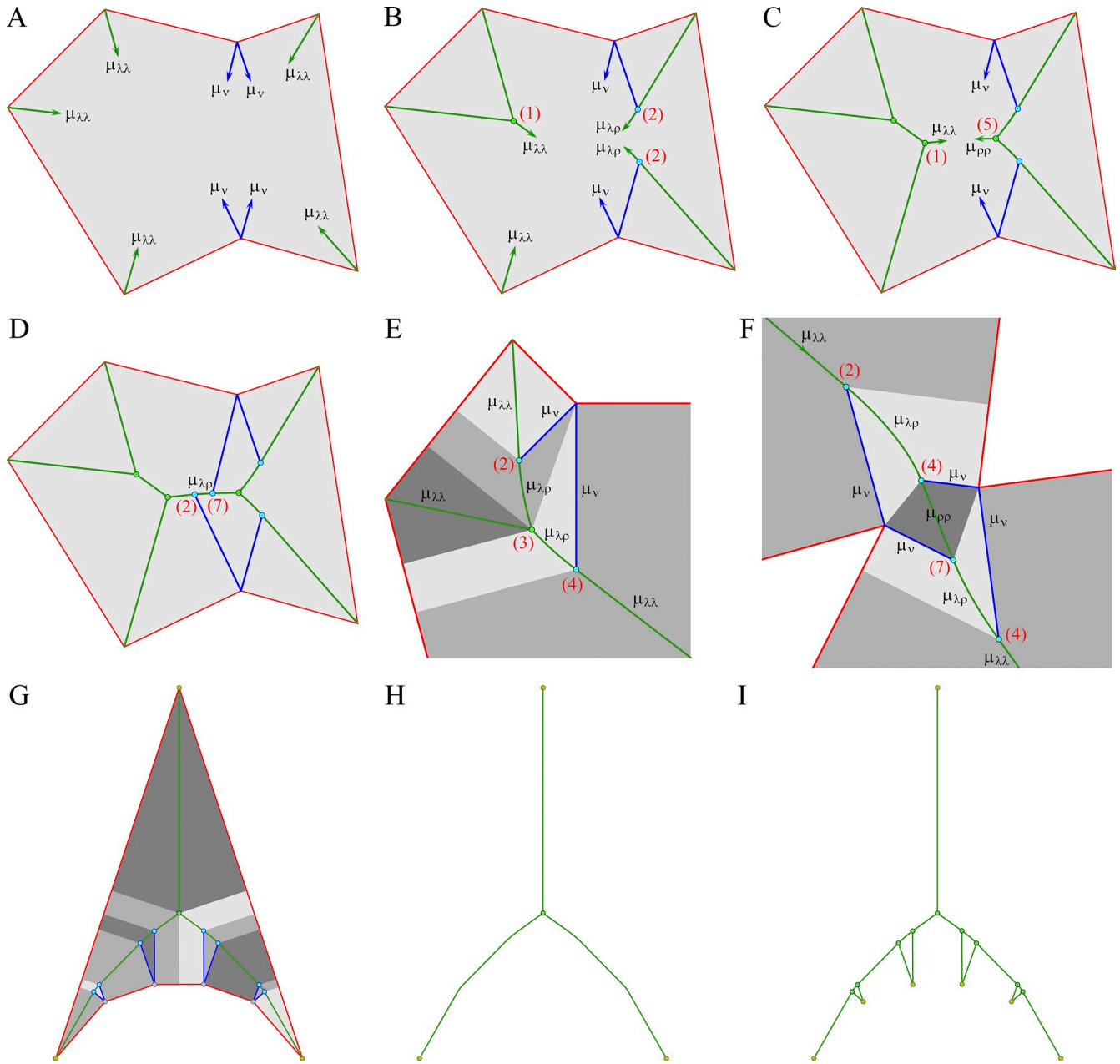
Figure S4. **Illustration of the collision algorithm and counting numbers of vertices and edges.** (A–D) Successive steps of the collision algorithm for constructing the Voronoi graph. Green lines and curves are the edges of the MAT ($\mu_{\lambda\lambda}$, $\mu_{\rho\rho}$, and $\mu_{\lambda\rho}$), and blue lines are remaining edges on the Voronoi graph (μ_ν). Any two colliding arrows produce a new arrow according to the rules 1, 2, 5, and 7 as marked in red. (E and F) A closer look at the collision rules 2, 3, and 4 and 2, 4, and 7, respectively. Adjacent gray areas of the same shade indicate regions bisected by the corresponding MAT edges. (G–I) Counting numbers of vertices and edges in Voronoi and medial axis graphs according to the expressions given in the Materials and methods. (G) Voronoi graph inside a polygon with three convex and four concave points. Adjacent gray areas of the same shade indicate regions bisected by the corresponding MAT edges. (H) MAT shown separately from the object boundary. (I) Voronoi graph shown separately from the object boundary.
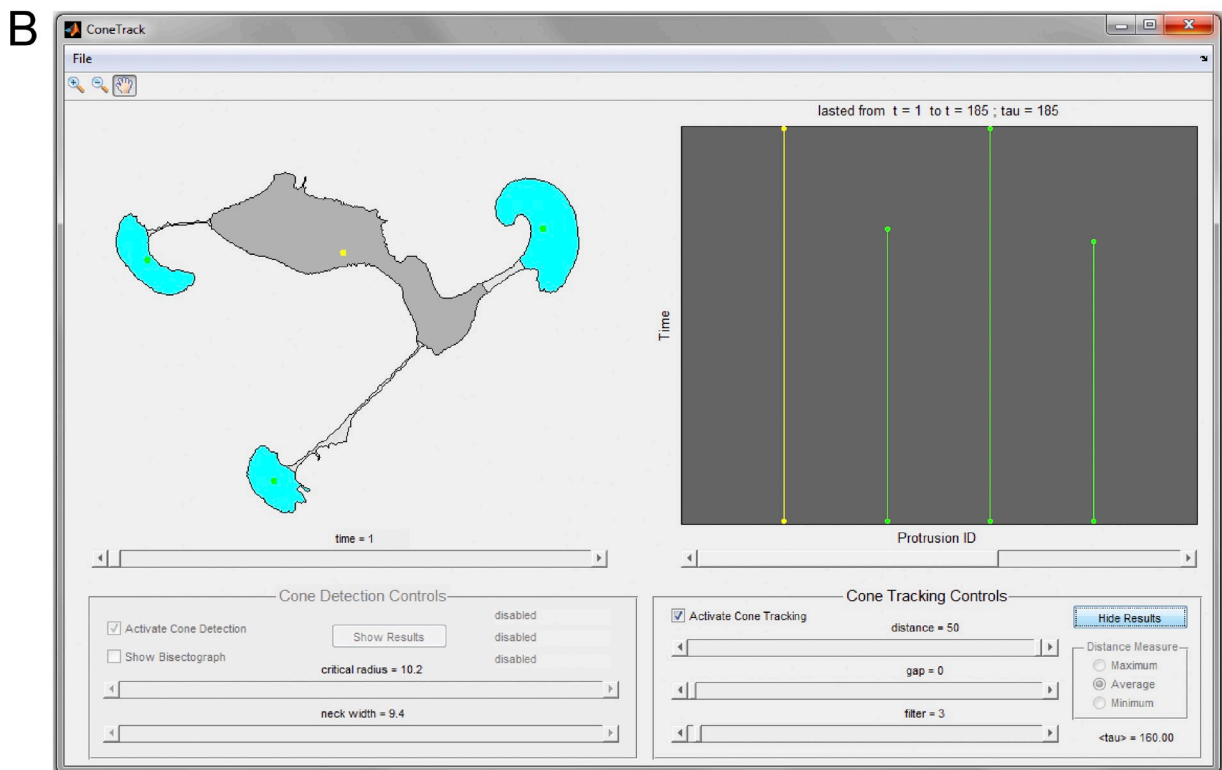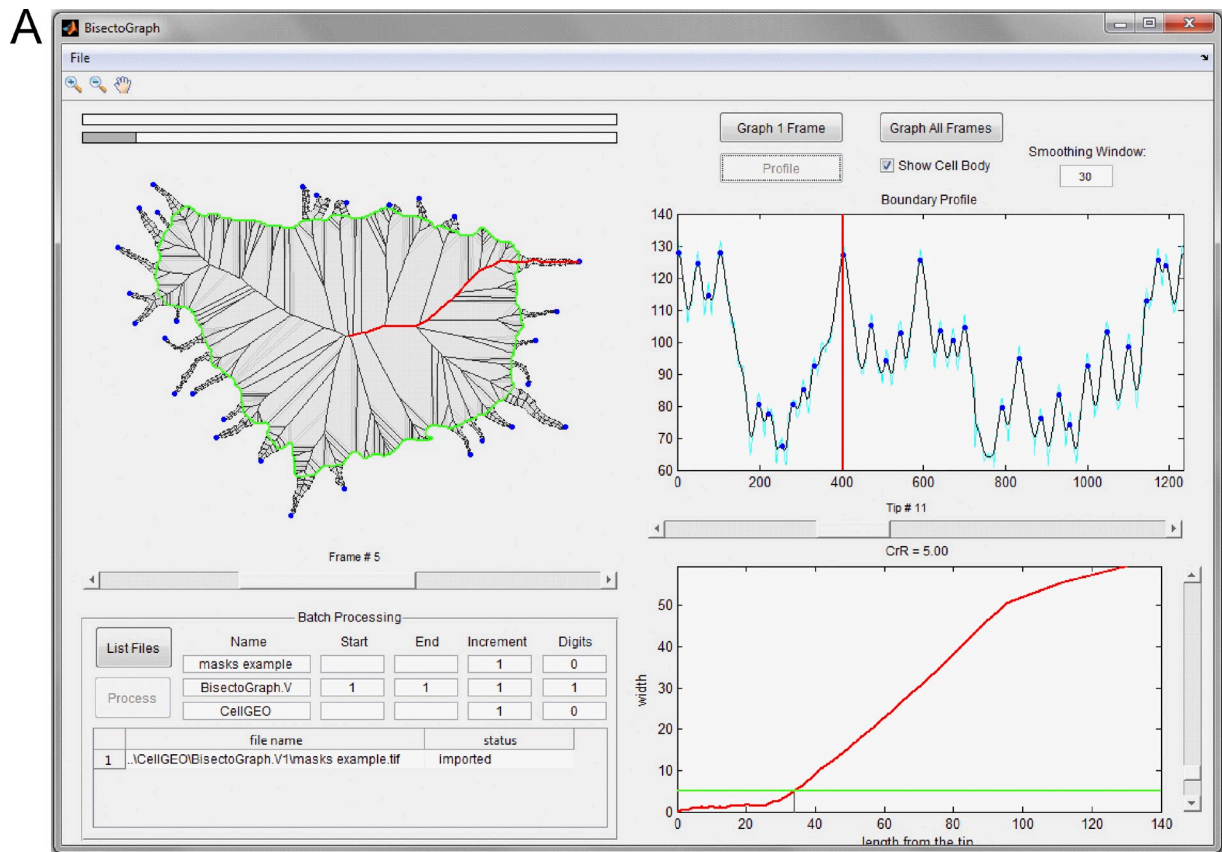
Figure S5. **Two screenshot examples of the GUIs.** (A) BisectoGraph module for finding tree graph representations of cell boundaries. The top left of the GUI shows boundary profiles with local maxima indicating protrusion tips (also shown as blue dots on the right panes). The bottom left shows width versus length $R(L)$ curve for a selected protrusion (red) and an adjustable critical width R_{cr} for protrusion base and cell body identification (green). (B) ConeTrack module for finding neuronal growth cones and cell body. The layout is the same as in FiloTrack (Fig. 5), but here, the sliders under the left section adjust the critical radius Ω_{cr} and neck width W_{cr}.
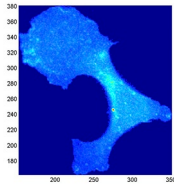
Video 1. **Medial axis interpretation as the ridges of the distance function.** The video visually illustrates one of the ways to understand MAT as a mathematical object by showing progressively a cell, its boundary, 3D view of the distance function, 3D view of the ridges, and 2D projection of the ridges (i.e., medial axis). Our actual algorithm does not involve the use of distance functions or ridges.
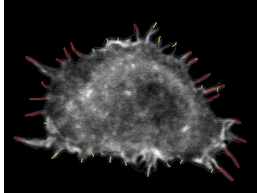
Video 2. ***Drosophila* D16C3 cell with a large number of filopodia identified using CellGeo.** A *Drosophila* D16C3 cell cotransfected with mCh-actin (white) and GFP-DiaΔDAD (not depicted) overlaid with the cell boundary (blue) and filopodia (red) after FiloTrack analysis. Protrusions are tracked and marked as longer (red) or shorter (yellow) than the critical filopodia length. Images were acquired by time-lapse confocal microscopy using a laser spinning-disc microscope (Wallac UltraVIEW; PerkinElmer) and 100×, 1.4 NA oil objective (Nikon). Frames were taken every 2 s for 7 min.
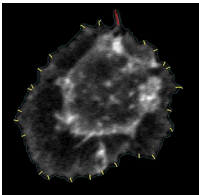
Video 3. **FiloTrack analysis of a *Drosophila* D16C3 control cell.** D16C3 cell transfected with GFP-actin and overlaid with the cell boundary (blue) and filopodia (red) after FiloTrack analysis. When protrusions are below the set critical filopodia length, FiloTrack marks them in yellow. Images were acquired by time-lapse confocal microscopy using a laser spinning-disc microscope (Wallac UltraVIEW; PerkinElmer) and 100×, 1.4 NA oil objective (Nikon). Frames were taken every 2 s for 3.5 min.
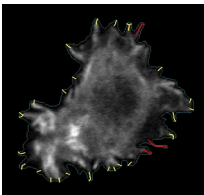
Video 4. **FiloTrack analysis of a D16C3 cell expressing constitutively active Dia.** D16C3 cell cotransfected with mCh-actin (white) and GFP-DiaΔDAD (not depicted) and overlaid with the cell boundary (blue) and filopodia (red) after FiloTrack analysis. Images were acquired by time-lapse confocal microscopy using a laser spinning-disc microscope (Wallac UltraVIEW; PerkinElmer) and 100×, 1.4 NA oil objective (Nikon). Frames were taken every 2 s for 3 min. When protrusions are below the set critical length, they are marked in yellow. Activated Dia increases the number and length of filopodia.

Video 5. **ProActive analysis of a D16C3 control cell.** Cell body movements after ProActive analysis of the D16C3 cell transfected with GFP-actin that is shown in Video 3. Images were acquired by time-lapse confocal microscopy using a laser spinning-disc microscope (Wallac UltraVIEW; PerkinElmer) and 100×, 1.4 NA oil objective (Nikon). Frames were taken every 2 s for 3.5 min. Filopodia are removed, and cell body outlines are overlaid to reveal cell body dynamics at a lag of 3, i.e., frame 1 is time t (red) and time $t + 3$ (blue), frame 2 is $t + 1$ (red) and $t + 4$ (blue), etc. Areas of protrusion are in white, and areas of retraction are in black.

Video 6. **ProActive analysis of a D16C3 cell expressing constitutively active Dia.** Cell body movements after ProActive analysis of the D16C3 cell transfected with mCh-actin and GFP-DiaΔDAD that is shown in Video 4. Images were acquired by time-lapse confocal microscopy using a laser spinning-disc microscope (Wallac UltraVIEW; PerkinElmer) and 100×, 1.4 NA oil objective (Nikon). Frames were taken every 2 s for 3 min. Filopodia are removed, and cell body outlines are overlaid to reveal cell body dynamics at a lag of 3, i.e., frame 1 is time t (red) and time $t + 3$ (blue), frame 2 is $t + 1$ (red) and $t + 4$ (blue), etc. Areas of protrusion are in white, and areas of retraction are in black. Activated Dia increases cell body protrusiveness.

Supplemental material also includes a ZIP file that includes the CellGeo package, which includes five folders corresponding to the five modules: MovThresh, BisectoGraph, FiloTrack, ConeTrack, and ProActive. Each folder contains MATLAB codes, data examples, and a text file with instructions on how to use the module (input format, output format, and processing steps).